Mon. Not. R. Astron. Soc. **000**, 1–?? (1996) Printed 1 February 2008 (MN LaTeX style file v1.4)

Starcounts in the Hubble Deep Field: Constraining Galactic Structure Models⋆

R. A. Méndez,[1] D. Minniti,[2,1] G. De Marchi,[1] A. Baker,[3,4] and W. J. Couch[3,5]

[1] *European Southern Observatory, Karl-Schwarzschild-Straβe 2, D-85748, Garching b. München, Germany*
[2] *Lawrence Livermore National Laboratory, MS L-413, P.O. Box 808, Livermore CA 94550, USA*
[3] *European Southern Observatory, Visiting Scientist*
[4] *Institute of Astronomy, Madingley Road, Cambridge, CB30HA, England*
[5] *School of Physics, University of New South Wales, Sydney 2052, Australia*

Accepted 1996 July 22. Received 1996 April 21

ABSTRACT

Stellar sources are identified in the Hubble Deep Field, and accurate colours and magnitudes are presented. The predictions of a Galactic starcounts model are compared with the faint stellar counts in this field. The model reproduces the observations very well in the magnitude range $21.0 < V \leq 26.4$, while it overpredicts the counts by a factor of four in the range $26.4 < V \leq 30.0$. The luminosity function for halo objects must be a factor of two smaller than that predicted by an extrapolation of the solar-neighborhood luminosity function for disc stars (with 95% confidence level). This result, seen before in deep Hubble Space Telescope images of globular clusters, is therefore confirmed for the halo field population. The possible nature of a group of faint-blue objects is also investigated, concluding that they are most likely non-stellar. The possibility that they are QSOs is ruled out. If we insist upon their stellar nature, they would be halo white dwarfs, with either a very steep halo white dwarf luminosity function for $M_v > +11.0$, or a stellar density 0.4 times that of the disc white dwarfs in the solar-neighborhood.

Key words: Galactic models – starcounts – halo luminosity function – halo white dwarfs

1 INTRODUCTION

The use of starcount models to constrain *global* Galactic structure parameters has proved to be an effective way of investigating the broad properties of stellar populations in our Galaxy (Reid and Majewski 1993). However, studies of the distribution at large distances above the plane require accurate photometry extending to faint magnitudes ($V > 20$), and such datasets are still rare (Majewski 1994, Robin 1994).

The faint end of the luminosity function (and its concomitant implications for the amount and nature of the local dark matter), is an important issue that can be resolved through starcounts to very faint magnitudes. A major obstacle in this area has been the difficulty in distinguishing faint images of stars from galaxies (which dominate the counts for $V > 20$), which has limited most of the ground-based work to $V \leq 20$. Only observations with a resolution higher than that imposed by the atmospheric seeing will be able to address these issues.

Recently, the Hubble Space Telescope (HST) has devoted 150 orbits in the continuous viewing zone to observe a high-galactic latitude field. This observation reaches very faint magnitudes ($V \approx 30$), and therefore can be used to explore starcounts to very faint magnitudes at the best resolution available. The observations in this so-called Hubble Deep Field (HDF, Williams et al. 1996) are analyzed in this article in the context of a galactic structure model. Constraints on the level of the halo luminosity function, and the nature of a population of faint-blue point-like objects detected in the frames is explored.

Sections 2 and 3 describe the assembly of the catalogue of stellar objects in the HDF. Section 4 compares the model predictions with the observed counts. Section 5 summarizes our main conclusions.

⋆ Based on observations obtained with the NASA/ESA Hubble Space Telescope, obtained at the Space Telescope Science Institute, which is operated by AURA, Inc., under NASA contract NAS5-26555.

2 THE HDF CATALOGUE OF SOURCES

The HDF object catalogue was created by running SExtractor (Bertin 1995) on the combined F606W and F814W frames, totalling 70 hours of exposure time. This combined frame provides the deepest exposure for detections at faint levels. Details of the catalogue creation can be found in Clements and Couch (1996). From this catalogue, a list of point-like objects was created by using the neural-network classifier within SExtractor that gives the probability of an object being point-like (in what follows this probability will be referred to as the "CLASS" of an object, with $CLASS = 0$ being an extended source and $CLASS = 1$ being a point-like object). This object selection is quite different from that presented by Flynn et al. (1996) and Elson et al. (1996) for the HDF data, in that we have used a non-linear, neural-network, multi-parameter classifier fed with basic image parameters. Despite the different selection criteria, our sample is almost identical to that of Flynn et al. (1996), judging from the similarity of the colour-magnitude diagrams. The reliability of the classifier has been demonstrated by Bertin (1994), and Bertin & Arnouts (1996).

Visual inspection of a subset of objects indicated that all objects with $CLASS < 0.85$ were clearly extended. This was used to create a list of sixteen possible stellar candidates for further inspection. SExtractor also measured magnitudes from the F300W, F450W, F606W, and F814W frames (however, most objects were too faint on F300W to be detected, see Table 1).

3 THE CATALOGUE OF STARS

Figure 1 shows the colour-magnitude and colour-colour diagrams for our sample of point-like objects. There appear two clumps of points, one resembling a faint main-sequence extension to low-luminosity stars, and a clump of blue, faint objects (these objects have also been reported by Flynn et al. 1996, their Figure 2). Figure 1a indicates the expected sequence of Population I main-sequence stars of different spectral type as seen through the HST filters. The blue objects mentioned before clearly depart from this sequence. Since all of these faint-blue objects had $CLASS = 0.85$ we suspected that they could be barely resolved galaxies. In order to test this hypothesis we created a histogram of the CLASS values to examine the distribution of classes. We found (Figure 2) that there is a broad local maximum at $CLASS = 0.80$ with wings extending to $CLASS = 0.85$ which suggested that the blue objects belonged to the same type of objects as the ones near this local maximum. We confirmed this by plotting the colour-magnitude and colour-colour diagrams for objects with $0.75 \leq CLASS < 0.85$ (all of which are extended objects as seen directly from the frames). These plots showed that the extended objects fall in the same region as the faint-blue objects found in our point-like sample. This suggests, therefore, that these objects are non-stellar. As a subgroup, these objects deserve special attention: We found that they *could not* be QSOs. Figures 1b-d indicate the locus of QSOs in the colour-magnitude and colour-colour diagrams from recent models by Baker (1995) for a range of possible QSO spectral indices and emission-line strengths. We also found (see next Section) that these objects could not be white dwarfs (WDs), unless the halo WD luminosity function is extremely steep.

When creating our point-like sample we found that a plot of CLASS *vs.* magnitude is not very informative because the overwhelming majority of detections are galaxies, not stars. With only 14 point-like objects and nearly 1500 galaxies spanning nearly 8 magnitudes of dynamic range, a plot like this does not indicate the reliability of the star-galaxy separation, nor it gives any information about the completeness of our stellar sample. We have found that a much better representation of the reliability of our star-galaxy separation is that given by the histogram of separations, shown in Figure 2. The validity of this procedure is confirmed by our numerical simulations (Section 4.1) and by two other independent results, namely those of Flynn et al. (1996) and Elson et al. (1996), as discussed below.

Additionally, the two brightest objects in our point-like sample were also excluded from the stellar list as these stars were saturated. Therefore, our stellar sample consists of eight objects in a field of view of 4.69 arc-min^2. Table 1 indicates the HST-STMAG instrumental magnitudes for both the stellar sample and the faint-blue point-like objects.

4 STARCOUNTS MODELING

Colour-magnitude and colour-colour plots in the Johnson-Cousins system are shown in Figure 3, where the faint-blue objects thought to be most likely extragalactic have also been included. Magnitude limits (for a 5σ detection of galaxies) have been determined to be 30.3, and 29.0 for the V and I filters, respectively (these magnitude limits are independent of colour in the range $1.8 \leq V - I < 3.0$). We should emphasize that we have *not* used colours at all to select our stellar sample. Our calibrated photometry is also presented in Table 1.

The paucity of objects fainter than $V \approx 26.2$ ($I \approx 24.4$) (well above the magnitude limit of our frames) is clearly seen in Figure 3a. This result is consistent with the findings by Flynn et al. (1996). We depart from their analysis in that we first *fit* a galactic structure model to the bright data, showing consistency with the model, and *then* we extrapolate to fainter magnitudes into the region where we do not observe any stars, to place constraints on the halo main-sequence luminosity function.

We use a galactic structure model that incorporates the three major contributors to the stellar counts in the solar neighborhood; a disc, a thick-disc, and a halo. Details of the model can be found in Méndez and van Altena (1996). For the most important parameter in this discussion, namely, the adopted halo luminosity function, we have used a M3-like luminosity function. This function has been constructed by padding the function of Sandage (1957) at the bright end ($M_v \leq 3.4$) with the Paez et al. (1990) function for fainter magnitudes. Beyond the Paez et al. completeness limit ($M_v \geq 7.4$) we have adopted the disc luminosity function for the solar neighborhood from Wielen et al. (1983). The function was scaled to a density of 0.15% of the stellar density at the solar neighborhood. The composite luminosity function has a ratio of $2.5 : 23 : 65$ at $M_v = 3.0 : 4.5 : 6.5$, similar to the best halo representation obtained by Reid and Majewski (1993).

Figure 1. Colour-colour and colour-magnitude diagrams in HST-STMAG instrumental magnitudes for all objects with $CLASS \geq 0.85$. Panel a) indicates the stellar sequence for spectral types A0 (bluest) to M8 (reddest). The bluest object at the bottom of the stellar sequence is saturated and not an A0 star. Panels b) to d) indicate the allowed range for the locus of QSOs depending on their power-law spectral indices and the strength of their emission lines. The locus has been computed from redshifts of $z = 0.1$ (bluest) to $z = 5.0$ (reddest).

Table 1. HST-STMAG and Johnson-Cousins photometry for our point-like sample.

ID	Chip	X	Y	F300W	F450W	F606W	F814W	V	B-V	V-I
1	2	1919.59	1913.17	23.610	21.717	21.528	21.715	21.11	1.05	0.70
2	3	1220.69	507.11	25.319	22.795	22.188	22.070	21.84	1.49	1.10
3	4	741.57	600.13	——	25.156	24.137	23.252	24.00	1.79	2.10
4	3	1055.63	1056.10	——	25.722	24.516	23.561	24.40	2.00	2.19
5	3	2003.79	1188.00	——	25.807	24.743	23.358	24.74	1.71	2.74
6	4	379.73	597.36	——	25.916	25.228	25.146	24.87	1.60	1.05
7	4	409.84	1580.44	——	26.858	25.652	24.951	25.46	2.07	1.86
8	2	1950.33	839.84	24.355	25.205	25.944	26.349	25.47	-0.03	0.41
9	2	976.68	1272.12	——	27.447	26.530	26.234	26.23	1.82	1.33
10	2	906.05	1694.03	——	26.123	26.926	27.549	26.40	-0.06	0.12
11	2	626.77	582.97	——	27.637	28.166	28.492	27.71	0.21	0.51
12	3	1026.22	813.84	——	27.498	28.106	27.973	27.77	-0.01	1.12
13	4	1789.74	1306.06	——	28.013	28.458	28.762	28.01	0.30	0.54
14	2	625.10	248.51	——	27.877	28.801	28.638	28.47	-0.41	1.16

Chip refers to the WFPC2 chip in which the object appears, while X and Y are the drizzled coordinates of the object (in pixels) on the respective Chip.

Figure 2. Distribution of classes. The distribution of classes reveals a clear separation between the local broad maximum at $CLASS = 0.80$ (extended objects) and a local peak at $CLASS = 0.94$ (point-like objects) in the form of a valley with very few objects in the range $0.88 \leq CLASS < 0.92$, indicating a good star-galaxy separation.

We have run the model in the magnitude range $21.0 \leq V < 26.4$ and $B - V > 1.0$ to match the colour and magnitude range of the observed counts (Figure 3a). The number of stars predicted by the model in the HDF field of view is 8.1 stars, while the observed number is 8. It should be emphasized that *no scaling whatsoever* has been applied to the model predictions, which are based purely on local values for the stellar density and local normalizations. We have found that variations in *all* of the model parameters (with the exception of the luminosity function) within their observational uncertainties have an effect smaller than the Poisson error in the observed counts (these parameters, e.g., scale-heights, scale-lengths, axial-ratio for the halo, etc., enter in a non-linear way into the model predictions).This implies that the predicted counts *are not* sensitive to the exact value adopted for these parameters and that any significant discrepancy between the model predictions and the observed value *has* to be attributed to the only remaining free parameter, namely, the luminosity function.

4.1 The halo main-sequence luminosity function

Figure 3a shows that in the range $26.4 \leq V < 30.0$ and $B - V \geq +1.5$) there are no observed objects. At $V = 30.0$ we are still 0.3 magnitudes above the 5σ magnitude limit (which pertains to galaxies with 16 connected pixels; the magnitude limit for point-like objects will be correspondingly fainter), and we expect to be fairly complete at this magnitude. Simulated images added to the HDF field indicate that the star-galaxy separation software is reliable to $V \approx I \approx 27.5$ and that the completeness at $V = 30$ is approximately 97% (L. Yan, private communication). The results of the extensive image simulations carried-out in the course of this investigation will be presented elsewhere (Reid et al. 1996). Here we only note that the question of misclassification is in our favor: since the overwhelming majority of objects in the HDF field are galaxies, any misclassification will likely bring more galaxies into this magnitude and colour range than the number of stars misclassified as galaxies. Diffuse and faint features associated with extended objects will not appear at the faintest magnitude levels, thus forcing the software to classify them as stars. This point has also been stressed by Elson et al. (1996), Section 2, and is clearly exemplified in their Figure 3. Since distinguishing point-like from extended sources requires approximately five times more photons than just detection (Flynn et al. 1996, Section 2), the above limit for reliable classification does imply that we can go much fainter than that for detection (as it is indeed found to be the case from our simulations). The basic point here is that, even if the classifier fails at $V \approx I \approx 27.5$, the non-detection of point-like objects fainter than that implies a true lack of stellar objects in this magni-

Figure 3. Colour-magnitude (panels (a) to (c)) and colour-colour (panel (d)) diagrams in the Johnson-Cousins system. The STMAG instrumental magnitudes were converted to the Johnson-Cousins system using the relationships by Holtzman et al. (1995). Since these conversions depend on colour, an iterative procedure was used to solve, simultaneously, for magnitudes in the three passbands B, V, and I.

tude range (as long as we are above the completeness limit). In this sense, the negative detection of point-like sources in this magnitude range is an *absolute upper limit* to the number of stars observed. Our high completeness at $V = 30$ (which is approximately of 97 %) is not surprising in view that the magnitude limit (5σ) for extended sources is 30.3 (as pointed out previously), implying that the corresponding 3σ limit for point-like detections is approximately $V = 31$. The magnitude limits for galaxies that we have quoted above have been provided by the STScI-HDF team.

The model predicts 6 stars in the range $26.4 \leq V < 30.0$ and $B - V \geq +1.5$, including 0.3 disc stars, 1.6 thick-disc stars, and 4.1 halo stars. The number of disc and thick-disc stars is formally consistent with no stars at all. The number of predicted halo stars is, however, larger than observed. This suggests that the true halo field luminosity function is a factor of four lower than implemented in the model. The mean distance (computed self-consistently from the model) for these halo stars is in the range 8.5 kpc (at $V = 26.5$) to 15.2 kpc (at $V = 29.9$). Therefore, the absolute magnitude range we sample is $+11.9 \leq M_v < +14.0$. In this magnitude range the halo luminosity function has been padded with the Wielen et al. (1983) function for the solar neighborhood, which reaches a maximum at, precisely, $M_v = +13.0$. We thus conclude that, at the 95% confidence interval, the halo field luminosity function is shallower, by a factor of two, than the Wielen function in this magnitude range, and that, most likely, it is a factor of four smaller. The small sample size, however, implies that this last statement is only a 2σ result, and that bigger samples would be needed to place stronger constraints. Also, with the present data we can not put constraints on the halo luminosity function at magnitudes fainter than $M_v = +14$. Our conclusion regarding the halo luminosity function coincides with recent findings by HST on the luminosity function of globular clusters (Paresce et al. 1995, De Marchi & Paresce 1995a,b). We should emphasize that, since the model already predicts 3.4 halo stars in the range $26.4 \leq V < 29.4$ and $B-V \geq +1.5$, the conclusions presented here regarding the halo luminosity function *are not* very sensitive to the exact magnitude limit of our sample of point-like objects. This also implies that the exact completeness fraction near the magnitude limit is less of a concern.

4.2 The white dwarf luminosity function

With the aid of the model we have explored whether the six faint-blue objects seen in the colour-magnitude diagram (with $V \geq 25$, $-0.5 < B - V < 0.5$ and $0 < V - I < 1.2$) could indeed be WDs. In the magnitude range $25.4 \leq V <$

27.8 and $B-V < 0.1$ we predict 15 objects per square degree, which would imply no stellar objects in our field-of-view. If we still assume that the objects we detect *are* WDs, it is instructive to see what this would imply in terms of their luminosity function. In one square-degree we would expect 1 disc WD, 2 thick-disc WDs, and 12 halo WDs. Therefore, if these objects are WDs, they would be halo WDs at distances of about 10 kpc from the sun. Excluding the two faintest objects in Figure 3 which could be misclassified galaxies (as found from our simulated images, see Section 4.1), we are left with 4 objects (note that at $V = 27.8$ we are well above the magnitude limit of our sample). This would imply that the halo WD luminosity function would have to be a factor of 260 times that of the disc (after normalizing to the density of halo stars in the solar neighborhood), or 0.4 times the local density of (disc) WDs. The mass density locked in halo WDs would be about $1.2 \times 10^{-4} M_{\odot}/pc^3$, which is, nevertheless, smaller by two orders of magnitude than the density required to explain the local circular velocity in the disc. Alcock et al. (1996) have recently suggested that a fraction of the dark halo could be indeed composed of halo WDs; the inferred masses from the latest microlensing events observed in the MACHO program towards the Large Magellanic Clouds are consistent with those of WDs. The alternative to just scaling the disc WD luminosity function would be to assume a very steep WD halo function for $M_v \geq +11.0$.

Besides the suggestion that this objects could indeed be unresolved galaxies (Section 3), another apparent difficulty with the WD scenario are the colours of these objects which differ by about 0.2 magnitudes from theoretical colours of Hydrogen and Helium WDs produced recently by Bergeron et al. (1995).

5 CONCLUSIONS

We find that a simple galactic structure model is able to reproduce the main-sequence starcounts to $V \approx 26.5$. There is an apparent lack of stars at fainter magnitudes, implying a halo field luminosity function flatter by, at least, a factor of two than the solar neighborhood Population I luminosity function in the range $+12 \leq M_v < +14.0$.

We also call attention to a group of faint and blue point-like sources. Their nature is most easily explained as being unresolved extragalactic objects (but not QSOs). On the other hand, if they are assumed to be stellar objects, they would most likely be halo WDs, implying a very steep luminosity function for these objects.

The papers by Elson et al. (1996), Flynn et al. (1996), and ours are three independent approaches to the study of the stellar sources in the Hubble Deep Field. There are similarities, dictated by the use of the same data set, but at the same time there are some important differences. We believe our paper is more quantitative in nature, using a recent Galactic starcount model (Méndez and van Altena 1996), and therefore it emphasizes the potential of these studies in the field of Galactic Structure and Stellar Populations.

In the paper by Flynn et al. (1996), they do not show that their bright stellar counts are in agreement with any Galactic structure model, which we do. This is an important step because it both validates the model, and permits a meaningful extrapolation to fainter magnitudes, which is important for establishing constraints on the halo luminosity function, as done in Section 4. On the other hand, their paper does not provide any light on the nature of the faint-blue objects which we also found. Their only remark about these extremely compact objects is that they would make it difficult to search for faint blue stars, and that they would investigate their possible nature. Instead, our analysis has shown that they could certainly not be QSOs, and that they are most likely not stars either. We have fully explored, though, the quantitative consequences of assuming that they are stars. We provide estimates of the effect of them being halo stars on the slope of the halo WD luminosity function, and the overall stellar and mass density of this objects in the solar vicinity. We have pointed out the resemblance of their CMD to ours, but we can not proceed any further in this comparison, since their paper does not contain a table indicating the photometric values for their stellar sample.

The analysis of the HDF starcounts in Elson et al. (1996) is more along the lines of our own analysis, with the following important differences:

(i) The Halo luminosity function: They compare the cumulative observed starcounts with models down to $V = 30$. We use the same magnitude cutoff based on our completeness tests, but we additionally break the sample into a 'bright' portion (where we do observe stars) and a faint portion (where we do not observe any stars). This separation of the sample into two subsamples is important as it permits different regions of the halo luminosity function to be mapped. For the bright sample the match to the model is perfect while for the faint sample there are discrepancies which lead to important constraints for the halo luminosity function as described in Section 4.1. We note also that Elson et al. have created their catalogue by using the F606W frames only, while we have created our list from the co-added F606W and F814W frames, allowing us to go deeper in terms of faint-level detections.

(ii) The faint-blue objects: Elson et al. discard the possibility that they are halo WDs mainly because since there are no such objects brighter than V= 26, these putative halo WDs would have to be located in a narrow shell at a distance of approximately 10 kpc from the Sun; certainly an unphysical solution. From our model, the distance distribution of these objects (should they be halo WDs) spans the distance range 7.8 kpc at V= 25.5 to 19.3 kpc at V= 27.7. They are not distributed in a thin shell, so this does not appear to be a good reason for discarding this model. In addition, as pointed out in Section 4.1, the fact that we do not observe blue objects brighter than $V \approx 26$ could actually imply a steep halo WD luminosity function which is not an unreasonable proposition in account of the older (and therefore cooler and redder) nature of the halo WDs. We provide also specific estimates to the corresponding mass density of halo WDs if these faint-blue objects are regarded as such.

Elson et al. discuss QSOs in the general context of their point-like sample by addressing mainly the expected *vs.* observed density of QSOs as a function of magnitude. Our approach is essentially complementary to theirs in that we actually compute the expected locus of QSOs, which lead us to discard the possibility that our faint-blue point like sample are QSOs. This, we believe, is an important contribution to understanding the true nature of this objects.

Summarizing, our analysis follows a logical sequence that makes the most use of the observations to constrain models, departing somewhat from the analysis by Flynn et al. and Elson et al., but providing complementary information about the nature of the sample of point-like objects found in the HDF. Despite our use of a completely different method for selecting stellar candidates we obtain a similar sample as that found by Elson et al. and Flynn et al.. This is quite reassuring, specially considering the difficulties inherent to create these samples at faint magnitude levels.

6 ACKNOWLEDGEMENTS

We have greatly benefited from conversations with Hans-Martin Adorf, Pierre Bergeron, Dave Clements, Stefan Dieters, Robert Fosbury, Markus Kissler-Patig, Francesco Paresce, Alvio Renzini. We specially thank Lin Yan for her contribution to the image simulations and the corresponding limits on completeness and star-galaxy separation. We would also like to thank the ST-ECF for arranging rapid access to the HDF data for European Astronomers.

REFERENCES

Alcock, C., Allsman, R.A., Alves, D.R., Axelrod, T.S., Becker, A., Bennett, D.P., Clayton, G.C., Cook, K.H., Freeman, K.C., Griest, K., Guern, J.A., Kilkenny, D., Lehner, M.J., Marshall, S.L., Peterson, B.A., Pratt, M.R., Quinn, P.J., Rodgers, A.W., Stubbs, C.W., Sutherland, W., & Welch, D.L., 1996, ApJ, to be submitted

Baker, A., 1995, Ph. D. Thesis, Cambridge University

Bergeron, P., Wesemael, F., Beauchamp, A., 1995, PASP, 107, 1047

Bertin, E., 1994, Astroph. & Space Sci., 217, 49

Bertin, E., 1995, SExtractor User Guide, pub. Institute d'Astrophysique, Paris

Bertin, E., and Arnouts, S., 1996, A&AS, 117, 393

Clements, D. L. and Couch, W. J., 1996, MNRAS, 280, L43

De Marchi, G., & Paresce, F. 1995a, A&A, 304, 202

De Marchi, G., & Paresce, F. 1995b, A&A, 304, 211

Elson, R. A. W., Santiago, B. X., and Gilmore, G. F., 1996, New Astronomy, in press

Flynn, C., Gould, A., and Bahcall, J. N., 1996, ApJ, 466, L55

Holtzman, J. A., Burrows, C. J., Casertano, S., Hester, J. J., Trauger, J. T., Watson, A, M., and Worthey, G., 1995, PASP, 107, 106

Majewski, S.R., 1994, In "Astronomy from wide-field Imaging", IAU Symposium No. 161, eds. H.T. MacGillivray, E.B. Thomson, B.M.Lasker, I.N. Reid, D.F. Malin, R.M. West, and H. Lorentz, Kluwer Academic Publishers, Dordrecht, p. 425

Méndez, R. A. and van Altena, W. F., 1996, AJ, 112, 655

Paez, E., Straniero, O., and Roger, C.M., 1990, A&AS, 84, 481

Paresce, F., De Marchi, G., & Romaniello, M. 1995, ApJ, 440 216

Reid, N., and Majewski, S. R.,1993, ApJ, 409, 635

Reid, I. N., Yan, L., Majewski, S., Thompson, I., Smail, I., 1996, AJ, in press

Robin, A.C., 1994, In "Astronomy from wide-field Imaging", IAU Symposium No. 161, eds. H.T. MacGillivray, E.B. Thomson, B.M.Lasker, I.N. Reid, D.F. Malin, R.M. West, and H. Lorentz, Kluwer Academic Publishers, Dordrecht, p. 403

Sandage, A., 1957, ApJ, 125, 422

Wielen, R., Jahreiβ, H., Krüger, R. , 1983, in The Nearby Stars and the Stellar Luminosity Function, IAU Colloq. No. 76, eds. A. G. Davis Philip and A. R. Upgren (L. Davis Press, Schenectady), p. 163

Williams, R.E., et al., 1996, AJ, in press

Table 2. Photometric differences between Flynn et al. (1996), Elson et. al (1996), and this work.

ID	ΔV_F	$\Delta(V-I)_F$	ΔV_E	$\Delta(V-I)_E$	$\Delta(B-V)_E$
1	0.09	0.18	——	——	——
2	0.27	0.19	-0.01	-0.13	-0.12
3	0.17	0.25	-0.29	-0.40	0.04
4	0.35	0.26	-0.15	-0.29	-0.07
5	0.18	0.14	-0.35	-0.51	0.13
6	0.16	0.27	-0.02	-0.13	-0.16
7	0.14	0.25	-0.17	-0.27	-0.02
9	0.19	0.31	-0.17	-0.16	-0.20
10	-0.02	0.04	0.09	-0.04	0.31
12	——	——	-0.11	-0.22	0.35

ID refers to our sequential number on Table 1. All the differences (Δ) are in the sense others - this paper. The subscript 'F' refers to the differences Flynn et al. (1996) - this paper, while the subscript 'E' refers to the differences Elson et al. (1996) - this paper.

7 NOTE ADDED IN PROOF

Subsequent to acceptance of our paper, Flynn et al. (1996) have been kind enough to provide us with their V and V-I photometric values. With these we have performed a comparison of theirs and Elson et al. (1996) photometry to ours. The results, for the objects in common among the three studies, are shown in Table 2 below. We find (see Table 2) that the mean differences (in the sense others - this work) are $\Delta V = 0.17 \pm 0.10$ and $\Delta(V-I) = 0.21 \pm 0.08$ with respect to the photometry by Flynn et al. (1996), while the mean differences for Elson et al. (1996) are $\Delta V = -0.13 \pm 0.14$, $\Delta(V-I) = -0.24 \pm 0.15$, and $\Delta(B-V) = 0.03 \pm 0.20$ (or $\Delta(B-V) = -0.06 \pm 0.12$ excluding objects 10 and 12 which belong to the possibly extended faint-blue sources). Our photometry seems to be midway between that of these other works. The origin of the discrepancy is unknown, but it can probably be traced back to the different methods employed to transform from the HST instrumental magnitudes to the Johnson-Cousins system. For example, Flynn et al. have used the transformation described in Bahcall et al. (1994, ApJ, 435, L51) which makes use of spectrophotometric standards to determine the zero-points and slopes of the conversion from the HST filters to the Johnson-Cousins V and I filters for each of the wide-field cameras. On the other hand, Elson et al. (1996) and ourselves use the calibration provided by Holtzmann et. al (1995). This explains why the difference in V and B-V between the photometry by Elson et. al and our work is negligible within the error bars. However, the large discrepancy in V-I is rather uncomfortable since the same transformations have been employed.

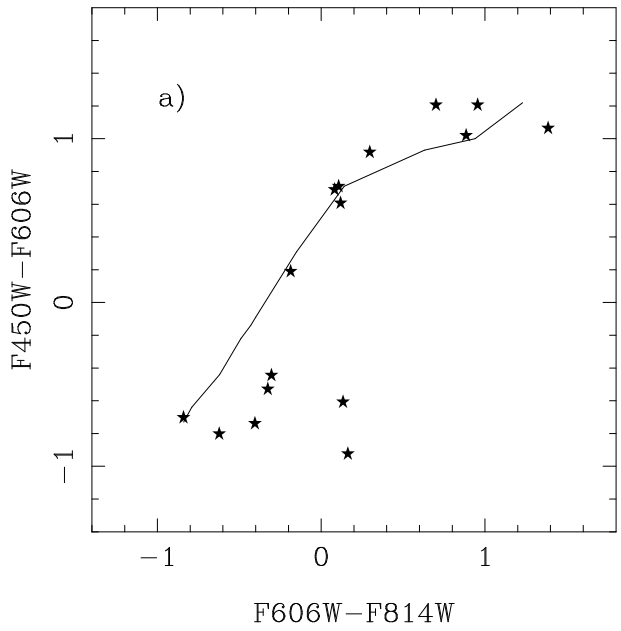
a)
F450W−F606W
F606W−F814W
−1
0
1

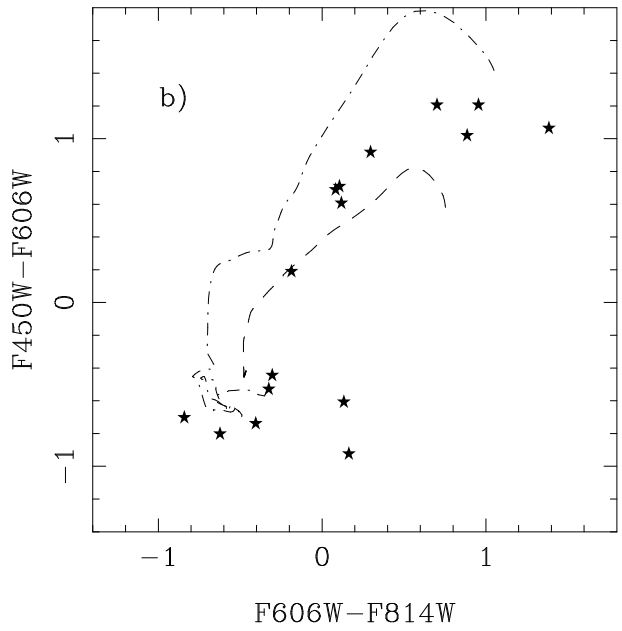
b)
F450W−F606W
F606W−F814W
−1
0
1

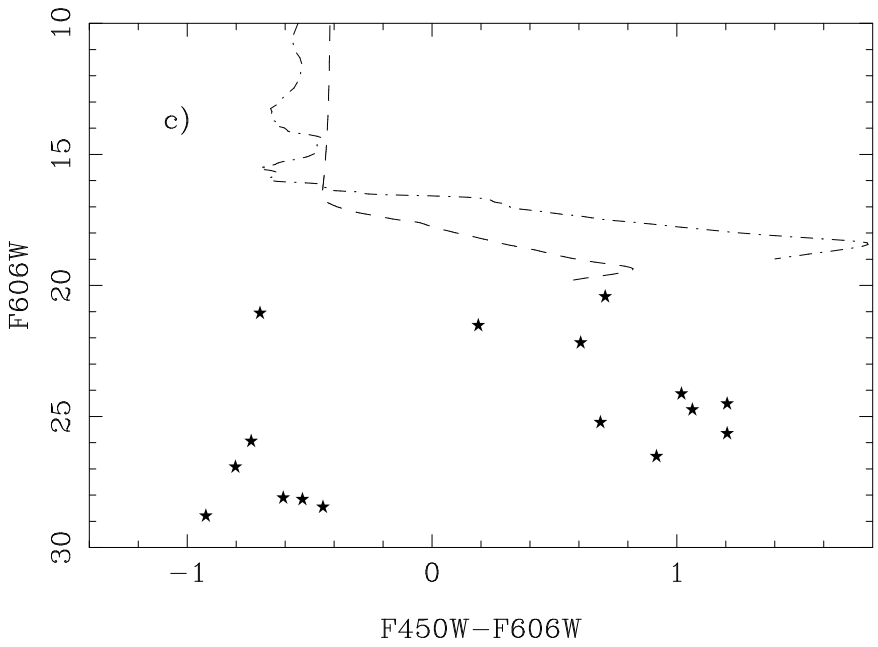
c)
F606W
F450W−F606W
10
15
20
25
30
−1
0
1

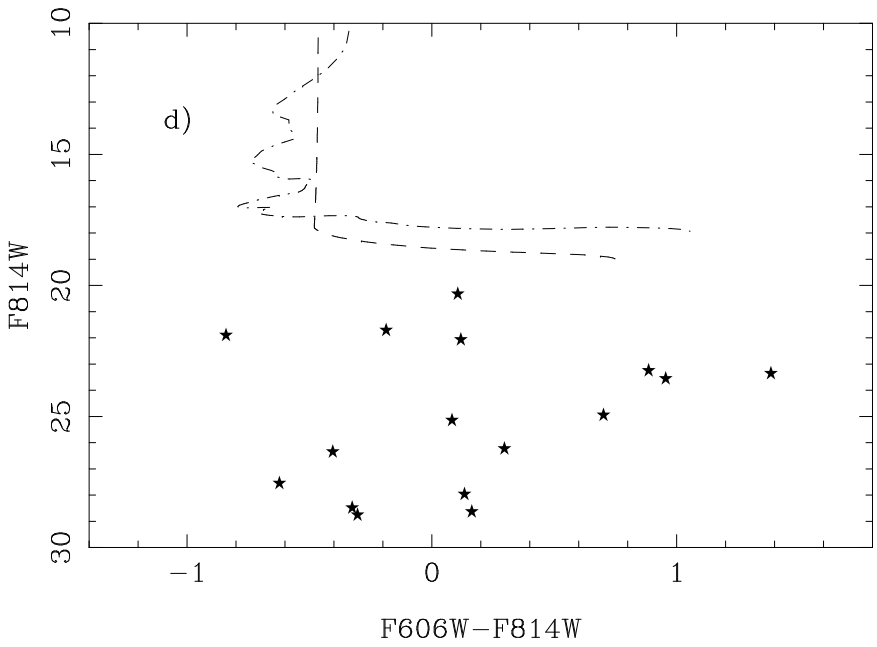
d)
F814W
F606W−F814W
10
15
20
25
30
−1
0
1

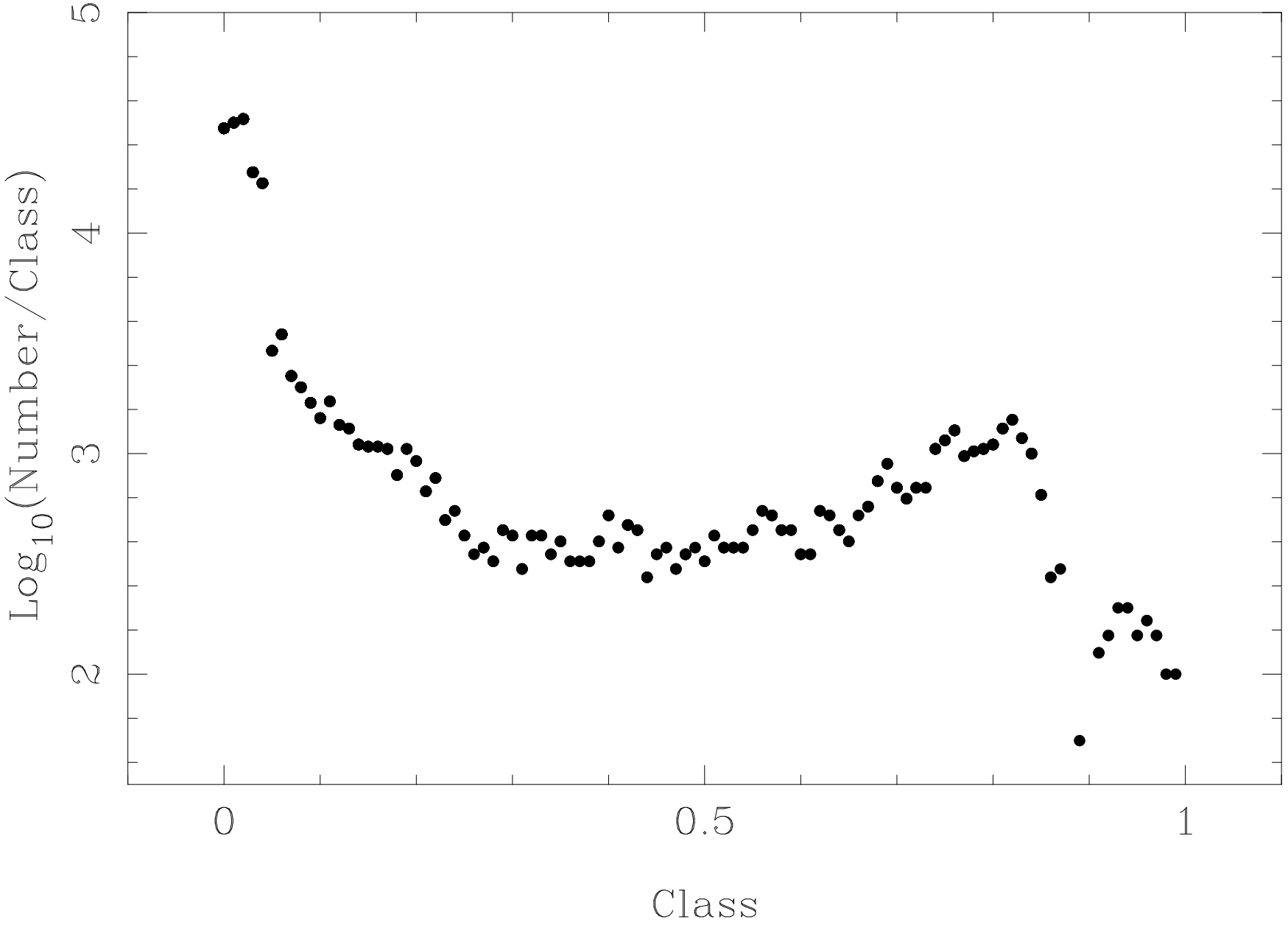
5
4
3
2
Log_{10}(Number/Class)
0
0.5
1
Class

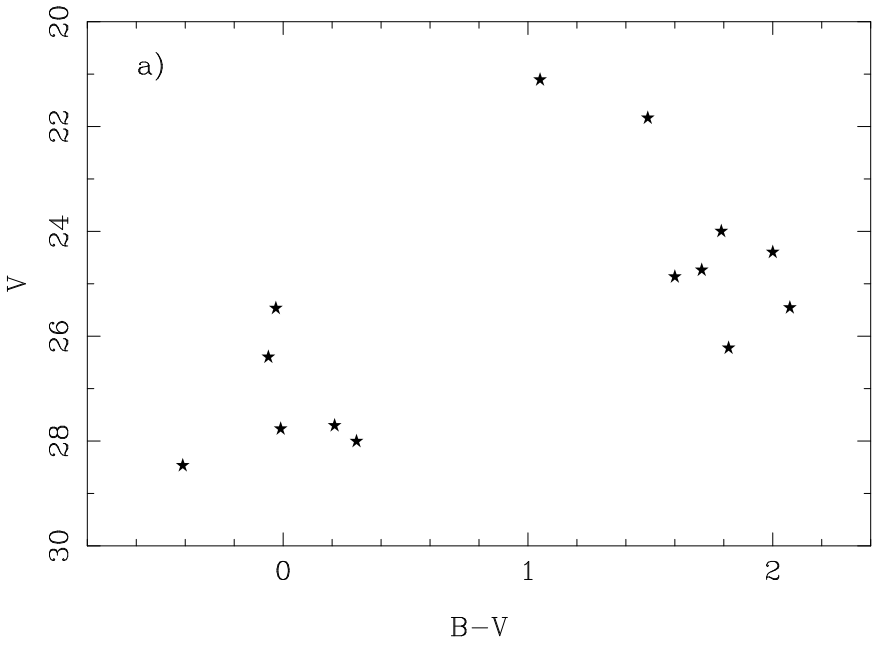
a)
V
B−V
20
22
24
26
28
30
0
1
2

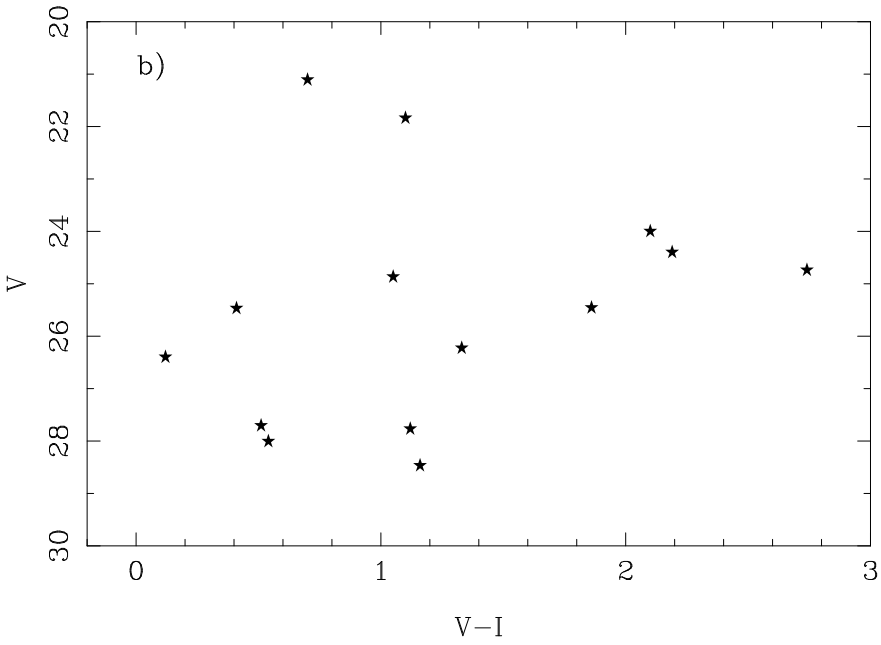
b)
V
V−I
20
22
24
26
28
30
0
1
2
3

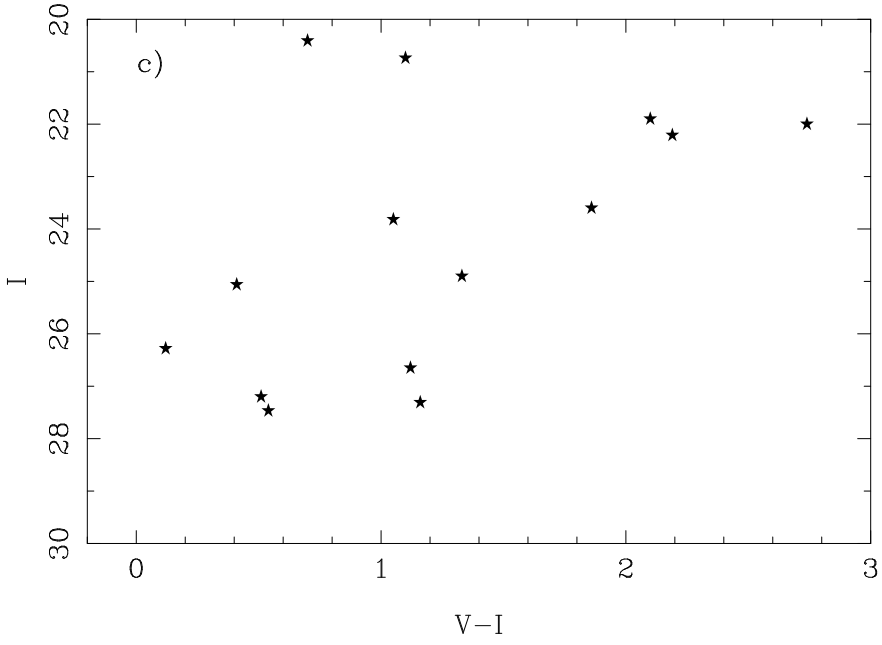
c)
I
V−I
20
22
24
26
28
30
0
1
2
3

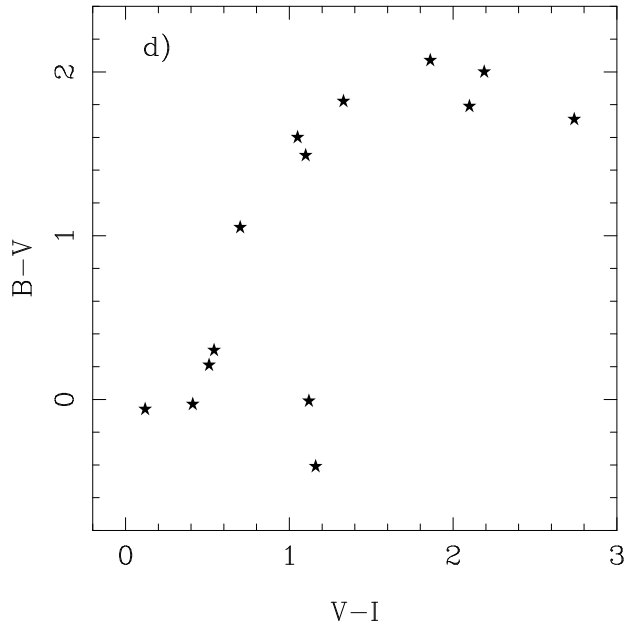
d)
B−V
V−I
2
1
0
0
1
2
3